UNIVERSITÀ DEGLI STUDI DI MILANO

DIPARTIMENTO DI
SCIENZE DELLA TERRA “ARDITO DESIO”

via Botticelli 23, 2013 Milano, Italy – Mauro.Giudici@unimi.it

Lecture notes

Physics of the hydrosphere and the cryosphere

Experimental and monitoring methods

Pumping tests

Exercises on ocean circulation and waves

Corso di Laurea Magistrale/MSc in Geophysics

Prof. Mauro Giudici

Academic Year 2023–24 — version January 2, 2024

Contents

Forward

These notes are a tutorial for the students, who attend the course unit “Physics of the hydrosphere and the cryosphere”, and cover some topics related to experimental and observation methods and some exercises related to groundwater flow and to ocean circulation and waves.

CHAPTER 1

Generalities on experimental and monitoring measures

1.1 General concepts about the measurement of physical quantities

1.1.1 Concepts related to the measurement quality

When an instrument is used to measure a physical quantity, it is impossible to avoid errors or uncertainties. For a comprehensive discussion of the treatment of errors and uncertainties on physical measurements, please, refer to Bevington (1969). Here only a few basic concepts used to quantify these limitations are recalled. In particular, here different terms, which in common language are often considered as synonyms, are defined in such a way as to differentiate them clearly.

Accuracy

Accuracy is defined as the difference ("error") between the measured value and the real value, whatever the latter is. Obviously, accuracy cannot be estimated in a perfect way, because the real value of a physical quantity is unknown (otherwise it would not be necessary to measure it!). Accuracy should be as low as possible and depends both on the instrument's quality and the correctness of measurement procedures.

Precision

Precision is defined as the, possibly random, spread of measured values around the average measured value. This is usually quantified by the standard deviation of repeatedly measured values of the same physical quantity. Precision depends mostly on the measuring instrument and should be as small as possible.

Notice that in geophysics and environmental studies, it is often difficult to repeat measurements of the same quantity under the same conditions. For instance, there is no possibility of repeating measurements for transitory phenomena like an earthquake or a tornado Therefore, it is often quite difficult to estimate the precision of a measurement.

Resolution

Resolution is defined as the smallest to be distinguished magnitude from the measured value. In other words, it is the smallest deviation from the measured value that can be assessed with a given instrument. Notice that the objective is to have the lowest value of resolution, even if in common language, this is referred to as “high resolution”.

Sensitivity

Sensitivity is the ratio between the variation of the quantity which is directly measured by the instrument and the variation of the quantity to be measured. For instance, in section 1.2.1 it is shown that the quantity which is directly measured with an amperometer is the torsion angle of a conducting wire loop and the value of electrical current is computed from this quantity. The objective of instrument design is to have high sensitivity. In fact, in that case, even a small variation of the quantity of interest could give an easily-measurable variation of the directly-measured quantity.

Measurement units

Finally it is important to stress that great care must be given to the use of proper measurement units. In particular, the definitions and the formats to be followed in order to be consistent with the International System of Units (SI) is managed by the Bureau International des Poid et Misures (BIPM)[1].

BIPM is an international organization established by the Metre Convention, through which Member States act together on matters related to measurement science and measurement standards. In particular, BIPM periodically updates a brochure, which provides instructions on the use of SI. Such instructions should be followed as precisely as possible both in scientific books and papers and in technical reports.

The ninth edition of the SI Brochure, which has been published in 2019, can be downloaded from the following `URL`:
`https://www.bipm.org/en/publications/si-brochure/`.

1.1.2 Experimental versus monitoring measurements

In geophysics and in environmental physics, it is important to distinguish between two kinds of measurements: experimental and monitoring measurements.

Experimental measurements are performed when all the conditions which might influence the measure are well controlled. This is the case in many experiments conducted in a laboratory. Instead, in geophysics and in environmental physics, it is more difficult to perform field measurements under perfectly controlled conditions.

The opposite condition corresponds to monitoring measurements, i.e., those measurements performed to assess the variation of a given quantity, possibly without control of the conditions by the operator. For instance, this is the case of stations to monitor air quality, where usually the concentrations of several contaminants are measured, but it is not possible to control the factors (e.g., traffic, house heating, etc.) which might influence the measured values.

1.1.3 Analog versus digital measurements

Analog measurements give a value which is based on the position of an indicator on a graduated scale. On the other hand, digital measurements provide discrete, numerical values.

[1]Details can be found at the web site `https://www.bipm.org/`.

In other words, analog measurements give values which vary with continuity in a given range, whereas digital measurements can give only values which vary in a discrete way. In principle digital measurements could give an infinite number of values, but in practice they are limited to a limited (possibly high) number of values.

Most physical variables can be considered as continuous quantities, in the sense that in principle they can assume any real value. Therefore, the quantities to be measured by an instrument should be considered as "analog" quantities. Digital measurements are then obtained by analog-to-digital conversion. This is performed with analog-to-digital converters (ADCs), whose basic characteristics are described in section 1.3. Here a couple of remarks only are given.

ADCs are based on two steps: sampling and holding (S/H) and quantizing and encoding (Q/E). In the S/H step, an analog signal is sampled with a regular sampling period ($\mathrm{T_S}$) and the value attained during a given time window (t_w) is held. In the second step, the held value is quantized, i.e., it is transformed into a numerical value in binary code. The resolution of an ADC depends on the range A, i.e., the difference between the maximum and the minimum values that can be released by the ADC, and on the number of bits N. In fact, the number of possible output-values given by the ADC are 2^N, so that the resolution is $A \cdot 2^{-N}$.

Improving the performance of an ADC requires both decreasing resolution by increasing N and increasing the sampling rate by decreasing $\mathrm{T_S}$. The effects of the sampling rate are discussed in section 1.1.4.

1.1.4 Aliasing

A time-varying analog signal can be considered as a function of time over a continuous domain. In other words, a continuous analog signal attains a value represented by any real number at any time, represented by a real number. When the continuous, analog signal is converted in a digital signal through an ADC, it becomes a discrete, digital signal, which means that the signal can attain only a finite number of values at specific, usually equally spaced, times. In other words, the continuous signal can be considered as a function of time with a continuous domain, whereas a discrete signal can be considered as a countable sequence of values, one value at each sampled time.

In this section, the effect of the discretization of the signal, i.e., of the ADC resolution, is not considered, whereas some remarks are given about the proper choice of the sampling rate. In fact, the transformation from a continuous to a discrete signal requires that ADC works at a sampling rate consistent with the characteristics of the original continuous, analog signal. In particular, the key problem is the relationship between the highest frequency of the spectral components of the original signal and the so called Nyquist frequency:

$$\nu_\mathrm{N} = \frac{1}{2\mathrm{T_S}}. \tag{1.1}$$

When a continuous signal is sampled with a given sampling period $\mathrm{T_S}$, it is possible to reconstruct the original signal in a perfect way from the discrete signal, only if the Fourier transform of the original signal is zero for $\nu > \nu_\mathrm{N}$. If this is not the case, the continuous signal which can be reconstructed from the discrete signal is distorted and components at high frequencies, i.e., for $\nu > \nu_\mathrm{N}$, are "reflected" at frequencies symmetrical with respect to ν_N, that it at $2\nu_\mathrm{N} - \nu$.

Without entering in the mathematical details of this fundamental result of the theory of discrete signals, figure 1.1 shows a simple case of a periodic signal, with frequency ν_0, and its reconstruction from sampling with three different sampling periods: $\mathrm{T_S} = (2\nu_0)^{-1}$ ($\nu_\mathrm{N} = \nu_0$; green line), $\mathrm{T_S} = \nu_0^{-1}$ ($\nu_\mathrm{N} = \nu_0/2$; blue line), $\mathrm{T_S} = 2 \cdot \nu_0^{-1}$ ($\nu_\mathrm{N} = \nu_0/4$; red line). It is apparent from this example that when the sampling period is so small that (1.1) is satisfied, then the

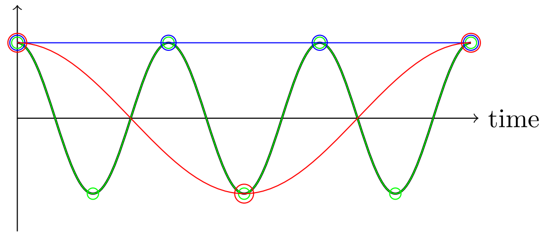

Figure 1.1: Example of the reconstruction of a continuous periodic signal with period T_0, after sampling at different frequencies: green line, $T_S = T_0/2$; blue line, $T_S = T_0$; red line, $T_S = 2T_0$.

original signal is perfectly reconstructed. On the other hand, if the sampling period is large, the reconstructed signal is evidently distorted. Figure 1.1 shows two pathological cases: when T_S is equal to the period of the original signal, the reconstructed signal is constant; when T_S is 1.5 times the signal period, the reconstructed signal is periodic, but its period is equal to 3 times the signal period.

1.1.5 Data storage and transmission

Data storage

Digital data can be stored in different types of memory systems, such as those which are used in almost any electronic equipment (PCs, smartphones, etc.). In geophysics and environmental physics, it is important to consider the storage requirements and the power needed to feed the sensors and the data storage system. In fact, monitoring sensors could be installed in positions with difficult access, far from electrical power lines and without the possibility of data transmission. Under these conditions, it is necessary to assess both the systems to provide energy (e.g., batteries fed by photovoltaic solar panels) and the capacity of storage devices, in order to limit the need of accessing the monitoring stations for data download.

A couple of examples can give an idea of the typical amount of data that have to be stored.

As a first example, consider a 16 bit ADC, with 10 channels, which permit to monitor 10 different physical quantities[2]. For a sampling period of 10 minutes, the rate of memory storage is given by

$$\begin{aligned}&24\,\mathrm{hour/day} \times 60\,\mathrm{minute/hour} \times 0.1\,\mathrm{sample/minute}\times\\&\times 10\,\mathrm{datum/sample} \times 2\,\mathrm{byte/datum} = 2,880\,\mathrm{byte/day} \simeq 2\,\mathrm{kB/d}.\end{aligned}$$

If the process is rapidly varying, so that it requires a small sampling period, e.g., 1 s, then the rate of memory storage becomes:

$$\begin{aligned}&24\,\mathrm{hour/day} \times 60\,\mathrm{minute/hour} \times 60\,\mathrm{sample/minute}\times\\&\times 10\,\mathrm{datum/sample} \times 2\,\mathrm{byte/datum} = 1,728,000\,\mathrm{byte/day} \simeq 1.6\,\mathrm{MB/d}.\end{aligned}$$

Therefore, quantities which vary at high frequency, might require specifically designed storage devices.

In some instances, it is possible to design and apply a triggered system. In this case, the data are sampled at high frequency, but they are stored for a given time window only when the signal amplitude overcomes a triggering threshold. This is very useful if the process to be monitored consists in a sequence of relatively short and rare episodes, which are nevertheless characterized by high-frequency signals.

[2] For instance, this could be realistic for a meteorological station.

Data transmission

Whenever possible, it is common practice that a network of sensors or monitoring stations or individual remote monitoring stations send acquired data to a control center for data collection. The control center might be relatively close to the network or the monitoring stations if a small area is monitored, whereas distances could be very large (up to tens of hundreds of kilometers) for monitoring stations located in isolated area with hard environmental conditions.

The designed system of data transmission strongly depends on the distances of sensors or monitoring stations from the control center, on the required rate of data transfer and on the availability of communication networks and electrical power lines close to the monitoring stations or sensors.

Radio transmissions are often used for this goal.

GSM coverage can permit the use of specific SIM cards to transfer data with an IP protocol.

Bluetooth systems can be used for data transfer in restricted areas.

1.1.6 Response time of a sensor

In order to introduce the concept of response time of a sensor, it seems useful the example of a sensor to measure temperature. If the sensor has being kept in contact with a body (or air, water or other natural materials) which has a steady temperature T_0, it attains this same temperature. If the temperature of the body changes instantaneously and reaches a value T_f, the sensor will not immediately reach the same value. The response of the sensor can be modeled by assuming that the rate of change of the sensor temperature is proportional to the difference between the temperature of the sensor and the body temperature:

$$\frac{\mathrm{d}T}{\mathrm{d}t} = \frac{T_\mathrm{f} - T}{\tau}, \tag{1.2}$$

where τ is called the response time of the sensor.

The solution to (1.2), is given by

$$T(t) = T_0 + (T_\mathrm{f} - T_0) \times [1 - \exp(-t/\tau)]\,. \tag{1.3}$$

From (1.3), it is apparent that after a time $t = \tau$, the difference between $T(\tau)$ and T_f is about 0.368 times the sharp temperature difference $T_\mathrm{f} - T_0$. Therefore, the smaller the response time, the faster the sensor will stabilize at the value to be measured.

1.2 Measurement of electrical signals (current and voltage) and resistance

1.2.1 Amperometer

Figure 1.2 shows the basic elements of an amperometer.

A conductive coil, consisting of N turns of a conductive wire is positioned inside the poles of a magnet, which is assumed to be realized in such a way as to produce a radial magnetic induction field $\mathbf{B}$ in correspondence of the vertical sides of the coil. If the electrical current to be measured, I, flows through the coil, then the interaction between the electrical current and the magnetic field yield a torsion moment, whose intensity can be computed as follows.

If the electrical current flows counterclockwise, then its direction along the vertical sides of the wire loop is perpendicular to the direction of $\mathbf{B}$, for the above assumptions. The direction of the force acting on each portion of the wire loop, according to the expression of Lorentz's

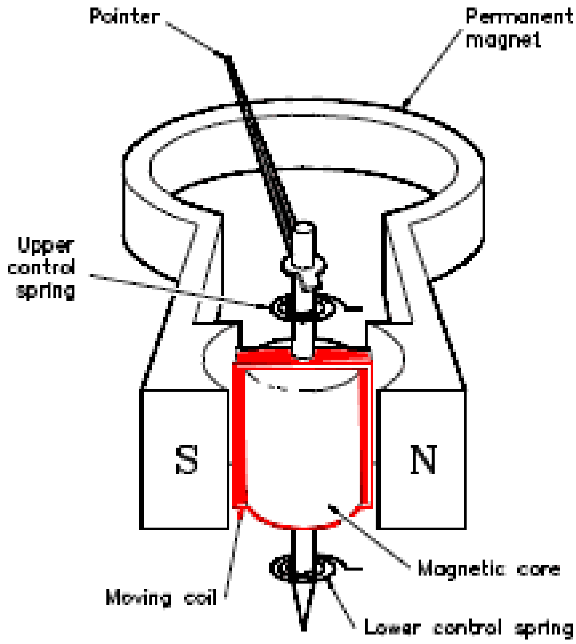

Figure 1.2: Sketch of the basic elements of an amperometer.

law for electrical currents flowing in conducting wires, is horizontal and tends to rotate the coil clockwise. The magnitude of the moment due to these forces is therefore given by:

$$M_{\text{mag}} = 2NLrBI, \tag{1.4}$$

where L is length of the vertical side of the wire loop, r is the "radius" of the wire loop, i.e., half of the horizontal side length, and $B = |\mathbf{B}|$.

The system is kept in equilibrium by the elastic torsion acting through the wire which sustains the wire loop and which tends to rotate the coil counterclockwise. The momentum of the elastic torsion is given by:

$$M_{\text{tor}} = C\theta, \tag{1.5}$$

where C is the constant of elastic torsion and depends on the geometry and the property of the elastic wire and θ is the torsion angle with respect to the equilibrium position of the coil when no electrical current flows in the instrument (i.e., in the wire loops).

At equilibrium, the intensity of both moments is equal, so that from (1.4) and (1.5), one obtains:

$$2NLrBI = C\theta. \tag{1.6}$$

From (1.6) it is clear that from the direct measurement of θ, I can be easily obtained, because N, L, r, B, and C are constructive parameters of the amperometer.

Notice that the sensitivity (see section 1.1.1) of this instrument is given by:

$$S = \frac{\Delta\theta}{\Delta I} = \frac{2NLrB}{C}, \tag{1.7}$$

where $\Delta\theta$ is the variation of the equilibrium angle for a variation ΔI of the electrical current. Equation (1.7) shows that sensitivity can be improved by increasing the number of loops, the dimension of the wire loop and the magnetic field, or by using a torsion spring with small C.

The conductive coil has a given resistance, R_a. This means that when the instrument is inserted in an electrical circuit where it is necessary to measure the electrical current, then a voltage difference $\Delta V = R_\mathrm{a} I$ appears at the two extremes of the amperometer. In other words, the amperometer itself becomes part of the electrical circuit and alters the current flows and potentials inside the circuit. In order to keep these perturbations as small as possible, R_a should be small. In practice, typical values of R_a are in the range between $1\,\Omega$ and $10\,\Omega$.

From the electrical point of view, the amperometer can be represented as shown in figure 1.3.

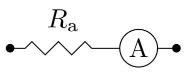

Figure 1.3: Scheme of an amperometer, as an element of an electrical circuit.

1.2.2 Voltmeter

An instrument with the same characteristics of the amperometer can be used also to measure potential differences. If R_v is the coil resistance, the potential difference is computed as

$$\Delta V = R_\mathrm{v} I = R_\mathrm{v} \frac{C\theta}{2NLrB}. \tag{1.8}$$

The basic difference with the case of the amperometer is that in this case one should reduce as much as possible the electrical current flowing through the voltmeter, which alters the current flow in the electrical circuit. Since the current I is inversely proportional to R_v, the above mentioned goal is achieved by using high resistances. In practice, typical values of R_v are not less than $1\,\mathrm{M}\Omega$.

In analogy with figure 1.3, figure 1.4 shows the scheme used to draw a voltmeter in the sketch of an electrical circuit.

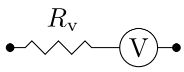

Figure 1.4: Scheme of a voltmeter, as an element of an electrical circuit.

Finally, the sensitivity of the voltmeter is obtained from (1.8) and is given by:

$$S = \frac{\Delta\theta}{\Delta V} = \frac{2NLrB}{R_\mathrm{v} C}. \tag{1.9}$$

1.2.3 Measuring resistances

In order to show examples of the use of amperometers and voltmeters and to discuss some other aspects, it is interesting and useful to examine different methods for the measurement of electrical resistances.

Volt-amperometric method

The first method that is considered, is based on Ohm's law. If a potential difference is applied to the resistance, then a given current flows through it and the measurement of the potential difference and of the electrical current permits to obtain the unknown value. This can be done with the circuit drawn in figure 1.5.

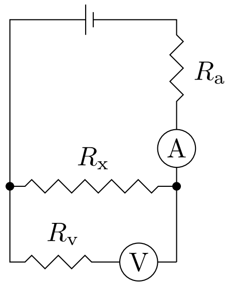

Figure 1.5: Electrical circuit for the measurement of resistance with the volt-amperometric method.

Let ΔV and I denote the measurements performed with the voltmeter and the amperometer. ΔV is exactly the potential difference across the resistance, whereas the actual current flowing through this element is given by $I_x = I - \Delta V \cdot R_v^{-1}$, because a portion of the current I flows through the voltmeter, which is connected in parallel with the resistance.

Therefore, the value of the resistance is obtained as follows:

$$R_x = \frac{\Delta V}{I_x} = \frac{\Delta V}{I - \Delta V \cdot R_v^{-1}} = \left(\frac{I}{\Delta V} - \frac{1}{R_v} \right)^{-1}. \tag{1.10}$$

Equation (1.10) explicitly shows the correction that accounts for the perturbation introduced by the measuring instruments, in particular by the voltmeter.

If $R_x \simeq R_v$, then the perturbation is excessive and the quality of the measurement could be low. In that case, an alternative electrical circuit for this kind of measurement can be used, as shown in figure 1.6. In this case $\Delta V = (R_x + R_a)I$ and therefore

$$R_x = \frac{\Delta V}{I} - R_a. \tag{1.11}$$

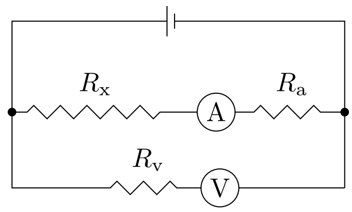

Figure 1.6: Electrical circuit for the measurement of high resistance with the volt-amperometric method.

Wheatstone and slide-wire bridges

Alternative methods for measuring resistances are based on the use of an electrical bridge. In this case, the measuring system is designed as a network of resistances and one of these resistances is changed until a null potential difference is established between two nodes of the network.

It is worth recalling that the measurement of a null value can be done with high quality. In fact, in that case, one can use a scale for the measuring instrument which is very small and the resolution is usually even much smaller. This should be clear, making reference to the formula which gives the resolution of a ADC, introduced in section 1.1.3: the resolution is proportional to the range of the instrument. If the value to be measured is small, then the measurement range can be very small and so the resolution.

Wheatstone bridge The first example is the Wheatstone bridge, shown in figure 1.7.

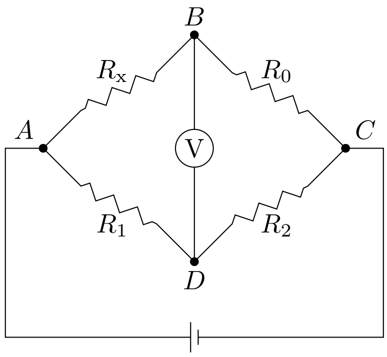

Figure 1.7: Electrical circuit for the Wheatstone bridge.

In order to measure R_x, R_0 is changed until $V_B = V_D$. Under these conditions, $I_0 = I_x$ and $I_1 = I_2$. Moreover, $V_C - V_B = R_0 I_0$ is equal to $V_C - V_D = R_2 I_2$, so that $R_0 I_0 = R_2 I_2$. Similarly, $V_B - V_A = R_x I_0$ is equal to $V_D - V_A = R_1 I_2$, so that $R_x I_0 = R_1 I_2$. From these formulas, it is easy to obtain

$$\frac{I_0}{I_2} = \frac{R_2}{R_0} = \frac{R_1}{R_x} \tag{1.12}$$

and finally

$$R_x = R_0 \cdot \frac{R_1}{R_2}. \tag{1.13}$$

In this case, the sensitivity of the instrument can be easily computed as

$$S = \frac{\Delta R_0}{\Delta R_x} = \frac{R_2}{R_1}. \tag{1.14}$$

Slide-wire bridge A similar approach is based on the use of a resistor, i.e., of an element with variable resistance. In particular, this can be thought of as a conductive wire, for which the second Ohm's law is applied, $R = \rho\mathcal{L}/\mathcal{S}$, where ρ is the resistivity of the material of the wire, $\mathcal{L}$ its length and $\mathcal{S}$ its section. The geometry of the bridge is shown in figure 1.8.

In this case, the point C separates the wire AB into two segments, whose lengths are a and b, so that $a + b = L$. The second Ohm's law implies $R_a = \rho a/\mathcal{S}$ and $R_b = \rho b/\mathcal{S}$. Equation (1.13) can be now applied by substituting R_1 with R_a and R_2 with R_b. As a consequence

$$R_x = R_0 \cdot \frac{a}{L - a}. \tag{1.15}$$

In order to compute the sensitivity, it is useful to express a as a function of R_x, from (1.15), i.e.: $a = LR_x \left(R_x + R_0\right)^{-1}$. Then the sensitivity can be computed as

$$S = \frac{\partial a}{\partial R_x} = \frac{LR_0}{\left(R_x + R_0\right)^2}. \tag{1.16}$$

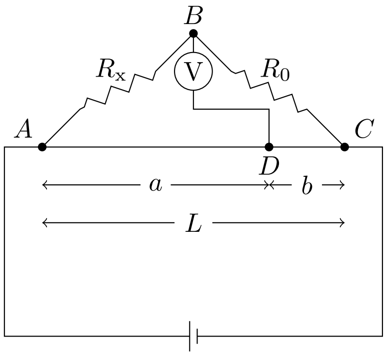

Figure 1.8: Electrical circuit for the slide-wire bridge.

1.3 Physical principles of ADCs

This section is devoted to a brief description of the basic physical properties of ADCs. ADCs are based on operational amplifiers (OpAmps). These electronic elements are also fundamental components of many electrical circuits. Therefore, some basic properties of these electronic components are presented and briefly discussed in the next subsection[3]. Finally, two examples of ADCs built with OpAmps are given.

1.3.1 Basic properties of operational amplifiers

Figure 1.9 shows the symbol of the operational amplifier used to draw electric circuits. The operational amplifier has two input nodes, called "non-inverting" and "inverting", and an output node.

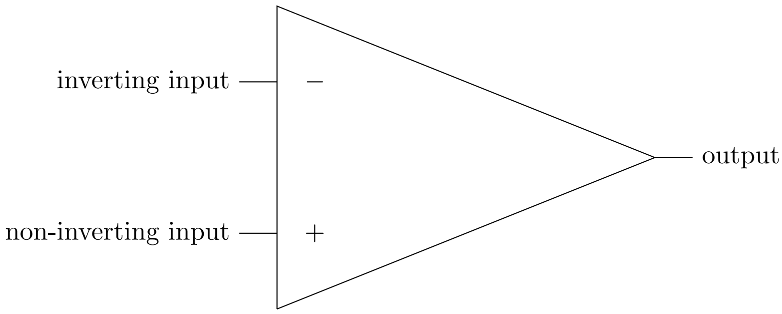

Figure 1.9: Symbol of the operational amplifier.

The ideal OpAmp

The operational amplifier has a complex behavior, which can be idealized by means of the sketch of figure 1.10.

[3]See `https://youtu.be/7FYHt5XviKc` for a video-tutorial covering some of the concepts described in these lecture notes.

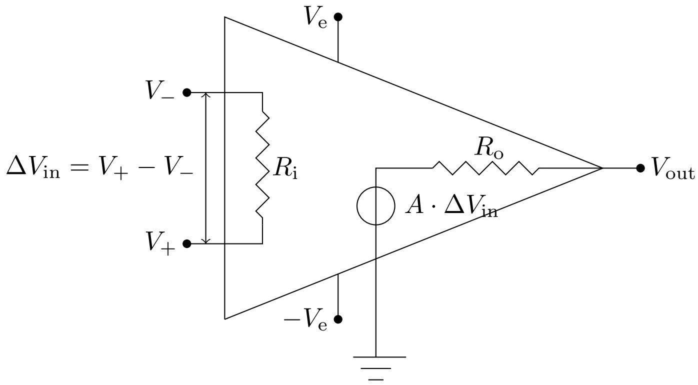

Figure 1.10: Scheme of the ideal operational amplifier.

The parameter A is called "open-loop gain" and represents the amplification of the input voltage difference. In order to permit such amplification, the device has to be fed by an external power system, with a voltage V_e.

The ideal amplifier is characterized by:

- $I_i = 0$, $V_+ = V_-$, $\Delta V_{in} = 0$;
- $R_i = +\infty$, $R_o = 0$; $A = +\infty$.

Typical values of real operational amplifiers are the following:

- $10^5 < A < 10^8$;
- $10^6\,\Omega < R_i < 10^{13}\,\Omega$;
- $10\,\Omega < R_o < 100\,\Omega$;
- $5\text{ V} < V_e < 24\text{ V}$.

The value of V_e sets a threshold for the amplified output voltage. In other words, it is possible to assume that the amplification is constant, up to a value $|A \cdot \Delta V_{in}| \leq V_e$.

Examples of simple circuits with OpAmp

In this subsection few examples of simple circuits are presented with two goals:

1. these examples are expected to help to understand the behavior of an operational amplifier;
2. the considered examples are used in the design and realization of ADCs.

Non inverting OpAmp Figure 1.11 shows a circuit, where an OpAmp is used in a non-inverting configuration. The current I circulates from the non-inverting node, where the electric potential is given by the source V_s, through R_i and R_o, to the node where the potential is given by $A\Delta V_{in}$. Therefore:

$$V_s - A\Delta V_{in} = (R_i + R_o)\,I. \tag{1.17}$$

By using the following relationship

$$\Delta V_{in} = R_i I, \tag{1.18}$$

equation (1.17) yields

$$V_{\mathrm{s}} = (AR_{\mathrm{i}} + R_{\mathrm{i}} + R_{\mathrm{o}})\, I. \tag{1.19}$$

Moreover

$$V_{\mathrm{out}} = A\Delta V_{\mathrm{in}} + R_{\mathrm{o}} I = R_{\mathrm{o}} I + AR_{\mathrm{i}} I = (R_{\mathrm{o}} + AR_{\mathrm{i}})\, I. \tag{1.20}$$

From (1.19) and (1.20), the following equation is obtained

$$V_{\mathrm{out}} = \frac{R_{\mathrm{o}} + AR_{\mathrm{i}}}{AR_{\mathrm{i}} + R_{\mathrm{i}} + R_{\mathrm{o}}} \cdot V_{\mathrm{s}}, \tag{1.21}$$

and finally, if the typical values of an ideal OpAmp are considered, the following final result is obtained:

$$V_{\mathrm{out}} \simeq V_{\mathrm{s}}. \tag{1.22}$$

In other words, the circuit of figure 1.11 permits to have an output voltage which "follows" the source voltage.

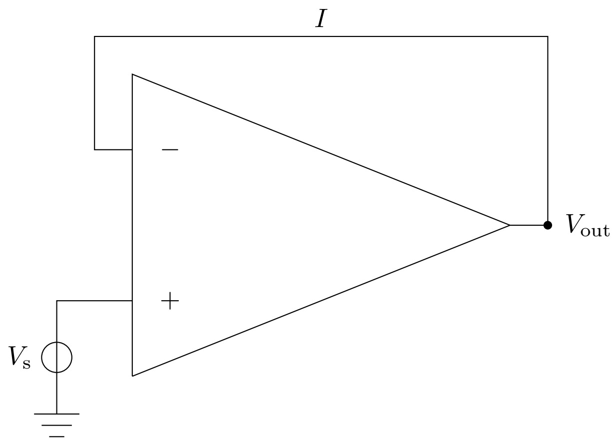

Figure 1.11: Non-inverting circuit.

Integrating circuit Figure 1.12 shows a circuit for the integration of the input potential.

The currents I_R and I_C flowing in the branches of the circuit are linked by the following relations:

$$-C\frac{\mathrm{d}}{\mathrm{d}t}\left(V_{\mathrm{out}} - V_{-}\right) = I_C = I_R = \frac{V_{\mathrm{in}} - V_{-}}{R}. \tag{1.23}$$

In the ideal case $V_{+} = V_{-} = 0$, so that (1.23) implies

$$\frac{\mathrm{d}V_{\mathrm{out}}}{\mathrm{d}t} = -\frac{1}{RC} V_{\mathrm{in}}, \tag{1.24}$$

which can be integrated to give

$$V_{\mathrm{out}}(t) - V_{\mathrm{out}}(0) = -\frac{1}{RC}\int_0^t V_{\mathrm{in}}(t')\mathrm{d}t'. \tag{1.25}$$

Therefore, the output signal is proportional to the integral of the input signal of the circuit.

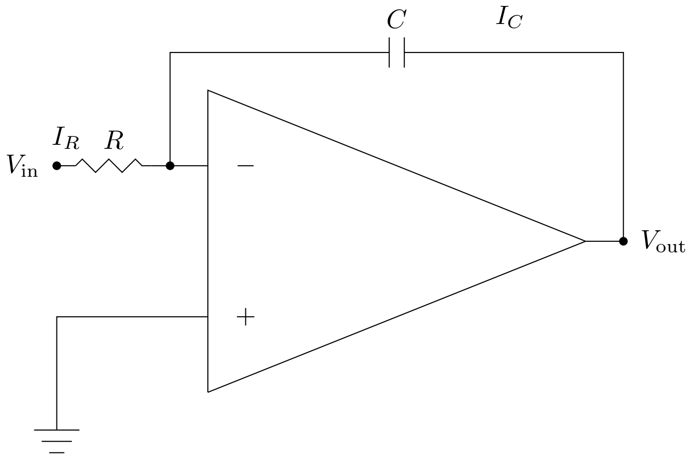

Figure 1.12: Integrating circuit.

1.3.2 Examples of ADCs

Two types of ADCs are illustrated here, as examples.

Flash ADC

Flash ADCs can be represented as a series of resistances, which are accompanied by a series of OpAmps: see figure 1.13 for a simple case of flash ADC with three bits.

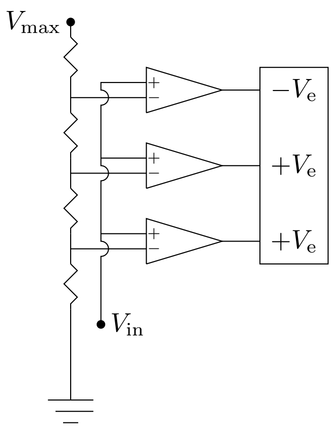

Figure 1.13: Scheme of a Flash ADC with two bits.

The total range (V_{max}) is subdivided in four steps, through a series of four resistances; the input signal is then connected to the inverting node of the OpAmp, whereas the midpoint between each couple of resistances are connected to the non-inverting node. With a proper choice of the OpAmps, each of them will provide a positive $V_{\text{out}} = +V_{\text{e}}$, if V_{in} is greater than the value at the non-inverting node, or a negative value otherwise. The example of figure 1.13 shows the case of a discrete signal, which corresponds to $V_{\text{max}}/2 < V_{\text{in}} < 3 \cdot V_{\text{max}}/4$. The resolution of the ADC is $V_{\text{max}}/4$.

Dual-slope ADC

OpAmps are often used in integrating circuits to design ADC with better performances. In this case, the integration proceeds for a time t_{int}. Then, a reference potential $-V_{\mathrm{ref}}$ is applied as input in order to lead the system again to a zero output voltage after an additional time $t_{\mathrm{de-int}}$; this stage is called the "de–integration" phase.

Therefore, the output potential is given by:

$$V(t) = \begin{cases} V_{\mathrm{in}} \dfrac{t}{\tau_{\mathrm{clock}}} & t < t_{\mathrm{int}}, \\ V_{\mathrm{in}} \dfrac{t_{\mathrm{int}}}{\tau_{\mathrm{clock}}} - V_{\mathrm{ref}} \dfrac{t - t_{\mathrm{int}}}{\tau_{\mathrm{clock}}} & t_{\mathrm{int}} < t < t_{\mathrm{int}} + t_{\mathrm{de-int}}, \end{cases} \tag{1.26}$$

where τ_{clock} is the characteristic time of the device, given by $\tau_{\mathrm{clock}} = RC$ for the circuit shown in figure 1.12.

At $t = t_{\mathrm{int}} + t_{\mathrm{de-int}}$, $V = 0$, so that

$$V_{\mathrm{in}} \frac{t_{\mathrm{int}}}{\tau_{\mathrm{clock}}} = V_{\mathrm{ref}} \frac{t_{\mathrm{de-int}}}{\tau_{\mathrm{clock}}} \tag{1.27}$$

and, eventually,

$$V_{\mathrm{in}} = V_{\mathrm{ref}} \frac{t_{\mathrm{de-int}}}{t_{\mathrm{int}}}. \tag{1.28}$$

Therefore the value of the input potential is obtained by the ratio among the times necessary for the integration and de–integration phases.

ADCs based on this principle are called dual-slope ADC, because the output voltage varies linearly during the integration and de–integration phases, but with different slopes: $V_{\mathrm{in}}/\tau_{\mathrm{clock}}$ in the integration phase and $-V_{\mathrm{ref}}/\tau_{\mathrm{clock}}$ in the de–integration phase.

CHAPTER 2

Measurement of oceanographic and hydrological quantities

2.1 Water level gauges

2.1.1 Point level detection

The direct measurement of water level is basically performed with three kinds of sensors.

1. Hydrometric rods[1], with which it is possible to visually measure the water level.
2. Phreatimeters, which consist of a graduated cable at the end of which is mounted a tip. The cable is lowered in a piezometer or in a standing well and when the tip touches the water, an electrical circuit is closed by water, so that an electrical current can be measured or an acoustic or luminous signal is activated.
3. Hydrostatic pressure sensors, usually piezoelectric sensors, which give an electrical potential difference proportional to pressure. These systems permit to measure, also in a continuous way and in unattended stations, the time variation of pressure at a given depth below the water level. Therefore, these gauges require the determination of the depth below a reference level (usually, the ground level) at which the sensor is installed and need to monitor the atmospheric pressure. The latter can be done, either by using cables[2] to keep one side of the sensor in contact with air at atmospheric pressure or by directly measuring atmospheric pressure close to the station where the water level is measured.

2.1.2 Non-contact level sensors

Non-contact measurement of water level is usually performed by means of ultrasonic methods. In other words, high-frequency (20 kHz to 200 kHz) acoustic waves are generated and they are reflected by the water surface. By measuring the two-way-traveltime necessary for the ultrasonic waves to reach the water table and come back to the receiver, after reflection, in principle it is easy to measure the distance of the water table from the sensor.

In order to perform high-quality measurements, some factors have to be carefully considered:

1. correction factors should account for the changing speed of sound due to moisture, temperature, and pressure variation in the atmosphere;

[1] "Stadia idrometrica" in Italian.

[2] These cables have to be reinforced because they must remain open even at some meters of depth, where the water pressure would cause them to get closed.

2. turbulence, foam, steam also affect the ultrasonic sensor's response;

3. proper mounting of the transducer is required to ensure the best response to reflected sound.

2.1.3 Stilling wells for tide monitoring

In principle, measurements of water level can be performed everywhere with one of the methods described in the previous sections. If the objective is tide monitoring, then it is important to filter high-frequency variations due to water waves or other perturbations. This is achieved by performing measurements in stilling wells. They essentially consist of relatively large wells, connected to the point where tide has to be monitored by a small pipe (figure 2.1). The high-frequency variation of pressure at the monitoring point does not propagate to the well where the water level is measured, as they are filtered out by the relatively small-diameter connecting pipe. The water level in the well can be measured with the above mentioned instruments.

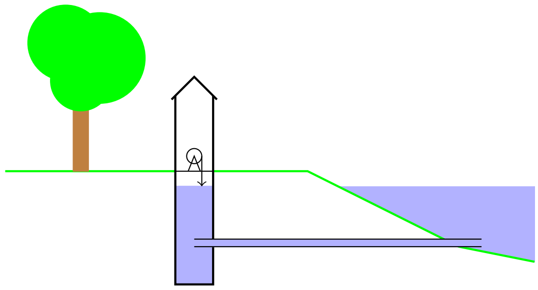

Figure 2.1: Scheme of a stilling well.

2.2 Wave buoys

Monitoring sea or lake conditions can be done by means of different systems of buoys.

1. Moored buoys range from 1.5 m to 12 m in diameter.

2. Drifting buoys are smaller, with a typical diameter ranging from 30 cm to 40 cm.

3. Weather buoys measure:
    - air temperature above the ocean surface,
    - wind speed (steady and gusting),
    - barometric pressure, and wind direction,
    - water temperature (usually at a depth of 3 m for fixed buoys),
    - wave height,
    - dominant wave period.

2.3 Current measurements

Current measurements are performed with two different approaches:

1. Lagrangian measures are based on the measurement of water parcels during their motion;

2. Eulerian measures are based on the measurement of water velocity at fixed positions.

2.3.1 Lagrangian measurements

Drifter are used to perform measures of sea currents. They consist of a float element with a drogue to facilitate the drifter to follow water movement and some waterproof containers for instruments. Drifters' position can be tracked by different systems, but satellite tracking and GPS positioning nowadays are common practice.

2.3.2 Eulerian measurements

Several methods can be applied to perform Eulerian current measurements.

1. Mechanical current meters are basically propellers.
2. An Acoustic Doppler Current Profiler (ADCP) measures the water current velocities over a depth range using the Doppler effect of sound waves scattered back from particles within the water column.
3. Electromagnetic induction can be used by some instruments. In fact, ions in seawater move with the ocean currents in the Earth's magnetic field and Faraday's law of induction permits to evaluate the variability of the averaged horizontal flow by measuring the induced electric currents.
4. Tilt current meters operate under the drag-tilt principle and are designed to either float or sink. A floating tilt current meter typically consists of a sub-surface buoyant housing that is anchored to the sea floor with a flexible line or tether. The housing tilts as a function of its shape, buoyancy (negative or positive) and water velocity.

2.4 Ocean vertical profilers

2.4.1 CTD (Conductivity-temperature-depth) sondes

CTD sondes consist of a cluster of sensors which measure conductivity, temperature, and pressure, which can be immersed or raised up from a ship (see figure 2.2). Other sensors to measure chemical or biological parameters (e.g., dissolved oxygen and chlorophyll fluorescence) may be added to the cluster. Sensors commonly scan at a rate of 24 Hz. Depth is derived from measurement of hydrostatic pressure, and salinity from electrical conductivity. Sensors are arranged inside a metal or resin housing; in particular titanium housings allow sampling to depths $> 10,000$ m. The following measurement procedure is usually applied:

1. immersion of the sonde to a determined depth or to a few meters above the ocean floor, generally at a rate of about $0.5\,\mathrm{m} \cdot \mathrm{s}^{-1}$;
2. during up-raising the rosette is stopped to collect water samples using attached bottles at depths based on the water column profile.

2.4.2 Nansen and Niskin bottles

Sampling water at different depths to perform measurements is done with Nansen[3] or Niskin[4] bottles (see figure 2.3, left and center). Water collection occurs by a rotation of the bottle when it reaches the designed depth for sampling. Since some of the parameters to be examined depend on

[3] After Fridtjof Nansen (1984).
[4] After Shale Niskin (1966).

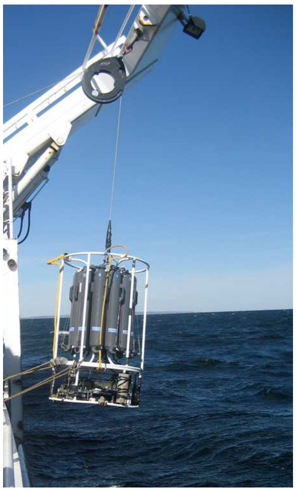

Figure 2.2: CTD sonde.

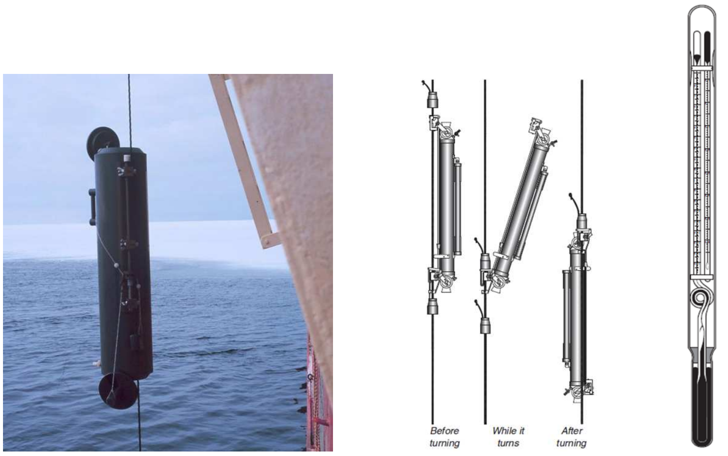

Figure 2.3: Picture (left) and scheme of work (center) of a Niskin bottle; reversing thermometer (right).

temperature, it is necessary to collect the temperature of water at the moment of sampling. This is performed with a reversing thermometer (figure 2.3, right). The latter consists of a mercury thermometer, which is built in such a way as to break the mercury column when reversed at the sampling depth. This prevents a relevant expansion of the mercury in the graduated column so that its extension remains fixed at the temperature at the moment of the sampling.

2.5 Bathymetry

Early techniques used heavy ropes or cables lowered over a ship's side. Modern instruments are sonars (SOund Navigation And Ranging), i.e., instruments which are based on the emission of a pressure (acoustic) wave which is scattered at the water body floor and bounces back to the recording instrument. From the two-way-traveltime, if the propagation speed of sound waves in water can be estimated properly (it is of the order of $1,500\,\mathrm{m}\cdot s^{-1}$), the depth of the water body floor beneath the water level can be obtained.

The typical frequency range is from 1 kHz to 30 kHz.[5]

Of course, precise assessment of bathymetry requires a knowledge of the physical conditions of water, e.g., temperature and salinity, in order to account for their effect on the speed of acoustic wave propagation. Moreover, the presence of extraneous bodies can cause spurious scattering, which should be avoided for accurate measurements. On the other hand, this is important for military and civil applications. In fact, sonars can be used to locate underwater bodies, like submarines or colonies of fishes.

Surveys with multibeam echosounders are nowadays quite common. These instruments consist of sonars which emit sound waves over a given fan in order to cover with a single emission a strip of water body floor.

2.6 Autonomous Underwater Vehicle (AUV)

AUV are becoming everyday more important in different areas. Besides their use in research and environmental monitoring, which is the most relevant for these lectures, their applications include:

- mapping seafloor for design of sub-sea infrastructure;
- pipeline inspection;
- control of illegal drug traffic;
- air crash investigations;
- military applications (UUV – unmanned underwater vehicles).

These vehicles are usually equipped with the following sensors: compasses, depth sensors, sidescan and other sonars, magnetometers, thermistors and conductivity probes, biological sensors (e.g., fluorimeters, i.e., chlorophyll sensors), turbidity sensors, and chemical sensors (pH, dissolved oxygen).

Positioning of AUV can be performed with different methods.

- Dead reckoning[6] is based on the knowledge of the initial position and of the speed and velocity direction of the AUV.

[5]Notice that audible sound has frequencies from 20 Hz to 20 kHz].
[6]"Navigazione stimata" in Italian.

- Long (LBL), Short (SBL) and UltraShort (USBL) BaseLine acoustic positioning systems are based on a framework of baseline stations, which must be deployed prior to operations and which determine the distances of the AUV with acoustic methods. SBL and USBL require the presence of a supporting ship.

Propulsion of AUV can be mainly given by three systems.

- Electrical engines connected with a propeller or thruster.
- Underwater gliders (figure 2.4) profit from variable-buoyancy propulsion, obtained by adjusting buoyancy either by using a piston to flood/evacuate a compartment with seawater or by moving oil in/out of an external bladder. In this case the typical motion is along an up-and-down, sawtooth-like profile, which permits to sample water parameters at different times and different positions.

Figure 2.4: Picture of an underwater glider.

- Wave gliders[7] are composed of two parts: the "float", roughly the size and shape of a large surfboard, travels on the surface of the ocean; the "sub" or wing rack hangs below on an umbilical tether whose length varies from 4 m to 8 m and is equipped with a rudder for steering and a thruster for additional thrust during extreme conditions (doldrums or high currents). The wave glider leverages the difference in motion between the ocean surface and the calmer water below to create forward propulsion.

2.7 Soil water content

Volumetric soil water content, θ, can be measured directly by means of the gravimetric method, which consists in collecting a soil sample, weighting it in humid conditions, heating it in an oven for a relatively long time, so that the contained water fully evaporates and weighting the dry sample. From the differences in weight of the wet and dry samples it is possible to determine the mass of water initially contained in the sample and eventually the water content.

Of course, this is a precise, but destructive procedure. A list of indirect methods of measurement of soil water content, follows.

1. Resistive probes are based on the measurement of the resistance of a gypsum block put in the ground; the gypsum will be in equilibrium with the soil and its water content will vary according to the variation of soil water content. If block resistance is calibrated against gypsum water content and a further calibration between moisture content in gypsum and in soil is available, then it is possible to infer the soil water content from the measured resistance.

[7] See `https://www.youtube.com/watch?v=77Wg1MFsLpQ&feature=youtu.be` for a video description.

2. Capacitive gauges are based on the remark that the relative dielectric constant (ϵ_r) of water is 80, whereas for most dry soils it varies from 2 to 5. From measurements of ϵ_r the soil water content can be inferred either by means of literature relationships[8], or by means of calibration for the specific soil under investigation. Two approaches for the measurement of ϵ_r are used.

   (a) TDR (Time Domain Reflectometry) applies a voltage pulse at one end of two (or three) conductive rods of length L, inserted in the soil (Figure 2.5). The voltage pulse travels along the rods and at the end, due to the discontinuity in electrical properties is reflected and is recorded back at the beginning of the rods after a time Δt. The speed of propagation of the electrical pulse is given by $c(\epsilon_r \mu_r)^{-1/2}$, where c is the speed of electromagnetic waves in air (or void), ϵ_r is the relative dielectric constant of the soil and $\mu_r \simeq 1$ is the relative magnetic permeability of the soil, which is close to one in absence of metal parts or ferromagnetic minerals. Therefore, $\epsilon_r = \Delta t^2 L^{-2} c^2 \mu_r^{-1}$.

Figure 2.5: Picture of a TDR probe.

   (b) FDR (Frequency Domain Reflectometry) is based on the measurement of the frequency at which a standing wave forms in the sensing device which is immersed in the terrain. Once again, this depends on the soil impedance and therefore on the soil electrical capacity and on ϵ_r.

Figure 2.6: Picture of a FDR probe.

3. Neutron probes use the property of fast neutrons[9] to be slowed down by collision with particles with the same mass as a neutron (i.e., protons, H^+). H_2O is the main source of H in most soils and, therefore, density of "thermalized" (i.e., slowed) neutrons formed around the probe is proportional to the volume fraction of water present in the soil.

4. NMR (nuclear magnetic resonance) application to the measurement of soil water content profits from the large nuclear magnetic moment of proton, i.e., of hydrogen. Resonance and relaxation processes in response to magnetic perturbations at radio-frequency is used to estimate the water content.

[8] One of the most used empirical formulas was proposed by Topp et al. (1980): $\epsilon_r = 3.03 + 9.3\theta + 146\theta^2 - 76.7\theta^3$ and $\theta = -5.3 \times 10^{-2} + 2.92 \times 10^{-2}\epsilon_r - 5.5 \times 10^{-4}\epsilon_r^2 + 4.3 \times 10^{-6}\epsilon_r^3$.

[9] Fast neutrons are emitted from a radioactive source (^{241}Am or ^{9}Be).

2.8 Suction

Figure 2.7 shows the ideal scheme of a tensiometer which could be used to measure matric potential in a partially saturated soil. With the notation of figure 2.7, $p_a = p + \delta g l$, where p_a is atmospheric pressure, δ is water density and g is the gravity acceleration. Therefore $p < p_a$ and $l = (p_a - p)/(\delta g)$. At point A, the water head is $h = z_A$. At point B, where there is equilibiurm between water in the porous cup of the tensiometer and in the soil, $h = z_B + \psi$, where ψ is the matric potential (or suction) at point B in the soil. As h is constant under equilibrium conditions, $z_A = z_B + \psi$, and since $l = z_B - z_A$ it is trivial to recognize that $\psi = z_A - z_B = -l$. In other words, l is the opposite of the matric potential. The scheme described above works for

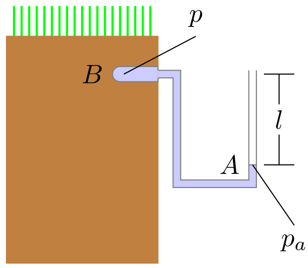

Figure 2.7: Scheme of a tensiometer.

$\psi > -10$ m, i.e., if $p > 0$, whereas it is not applicable for absolute values of ψ greater than 1 atmosphere.

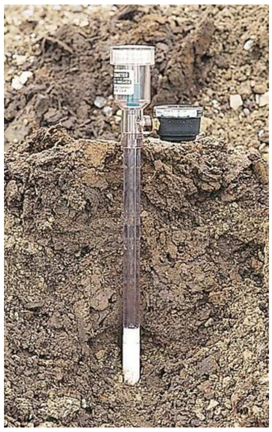

Figure 2.8: Picture of a tensiometer.

CHAPTER 3

Exercises for groundwater flow

3.1 Interpretation of pumping tests

During a constant flow pumping test, the values of drawdown as a function of time are detected in a piezometer placed at a distance r from the well, which withdraws water from the aquifer at a constant flow rate Q. Calculate the values of the transmissivity T and of the storage coefficient S with the Theis and Jacob method.

3.1.1 Solution with the Theis method

The Theis equation provides the temporal trend of the lowering of the water table as a function of time:

$$s(r,t) = \frac{Q}{4\pi T} W(\eta), \tag{3.1}$$

where the dimensionless variable η and the function W, called "well function", are defined by:

$$\eta = \frac{Sr^2}{4Tt} \tag{3.2}$$

and

$$W(\eta) = \int_{\eta}^{+\infty} \tau^{-1} e^{-\tau}\, \mathrm{d}\tau. \tag{3.3}$$

The integral that defines the well function is a remarkable integral of the mathematical analysis which is called the "exponential integral" and can be calculated through a series expansion:

$$W(\eta) = -\gamma - \ln(\eta) + \eta - \frac{\eta^2}{2!\,2} + \frac{\eta^3}{3!\,3} - \frac{\eta^4}{4!\,4} + \dots, \tag{3.4}$$

where $\gamma = 0.5772157$ is Euler constant.

To compare the experimental data with the theoretical curve, it is convenient to work with the dimensionless variable u defined by:

$$u = \frac{1}{\eta}. \tag{3.5}$$

The well function has the trend shown in figure 3.1 as a function of u.

If the experimental data (drawdown vs time) are displayed in a log-log scale, they are represented as points whose trend is similar to the curve in figure 3.1. Obviously, the points do not fall

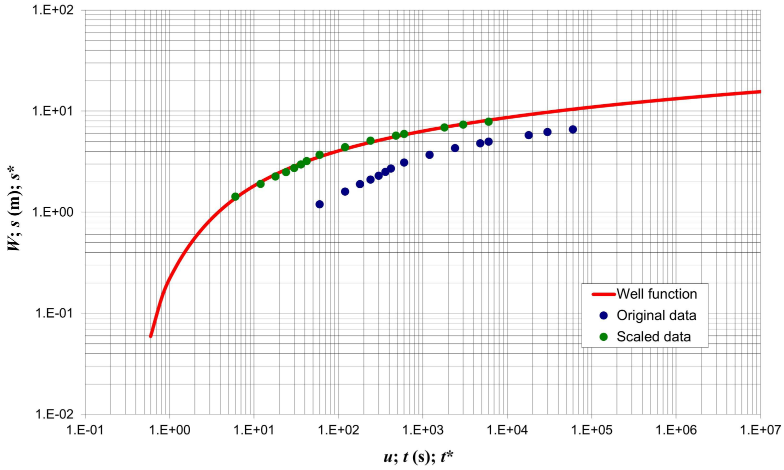

Figure 3.1: Graph of the well function as a function of u and comparison between experimental data and theoretical curve. Notice that the absolute values of W, s, and s^* are represented here, in order to draw them with a log-scale.

on the theoretical curve. Notice that the drawdown vs time plot is a dimensional graph, while the W vs u plot refer to dimensionless quantities. To compare the experimental data with the theoretical curve it is necessary to make time and drawdown dimensionless. For this purpose the variables t and s must be multiplied by two constants A and B given by:

$$A = \frac{4T}{Sr^2}, \quad B = \frac{4\pi T}{Q}. \tag{3.6}$$

In this way, dimensionless quantities t^* and s^* can be defined:

$$t^* = A \cdot t, \quad s^* = B \cdot s. \tag{3.7}$$

Since T and S are unknown, it is necessary to proceed, e.g., by trial and error, until the values of the coefficients A and B, which allow the experimental points to fall on the theoretical curve with the best possible precision, are obtained (figure 3.1). The multiplication of t and s by two constants acts on the log-log scale graph as a horizontal and vertical translation.

Once a good agreement has been obtained between the theoretical curve and the experimental data expressed through the dimensionless variables, the coefficients A and B can be used to calculate the transmissivity and the storage coefficient from equations (3.6).

3.1.2 Solution with the Jacobi method

When t is large, so that η is small, (3.4) yields

$$W(\eta) \sim -\gamma - \ln(\eta), \tag{3.8}$$

so that

$$s(r,t) \sim c - \frac{Q}{4\pi T} \ln\left(\frac{Sr^2}{4Tt}\right), \tag{3.9}$$

where $c = (Q\gamma) \cdot (4\pi T)^{-1}$.

Therefore, for long times, the drawdown follows a linear trend as a function of $\ln t$, so that the values of T and S can be inferred from linear regression of s vs $\ln t$.

3.1.3 Problem 1 - Confined aquifers

With the data from one of the three examples listed in sheet `Confined aquifers` of the file `PumpingTests.xls`, estimate T and S with Theis' method.

3.1.4 Problem 2 - Phreatic aquifer

Sheet "`Phreatic aquifer 1`" of file `PumpingTests.xls` lists the data measured during a pumping test in a phreatic aquifer. In particular, the drawdown in the well and in five piezometers are given. Assuming that T can be approximated as independent of h, estimate T and S with Theis' method. Discuss the conditions under which the above mentioned assumption is satisfied.

3.1.5 Problem 3 - Phreatic aquifer

Sheet "`Phreatic aquifer 2`" of file `PumpingTests.xls` lists the data measured during a pumping test in a phreatic aquifer. In particular, the sheet includes:

- data about the well test and the well characteristics (columns A to D);
- the pressure (expressed as a water level in meters) and the temperature measured by a sensor installed at a certain depth in the well (columns F to M);
- the pressure (expressed as a water level in meters) and the temperature of the air outside the well, measured by a sensor (columns O to V).

The test lasted some days and the data show:

- some effects related to the installation of the equipments;
- a sudden drawdown when the pump is turned on (in the morning) and a sudden recovery of the water level when the pump is turned off (in the evening).

The processing and interpretation of the data should consider the following steps:

1. determine the variation with time of the water level in the well, by correcting for the variation of atmospheric pressure;
2. isolate from the whole time series the data which refer to the drawdown and the recovery phases;
3. apply Theis equation for both phases (drawdown and recovery) and estimate the values of T and S.

3.2 Tide effects on the water level in a coastal aquifer

3.2.1 The data set

The data considered for this example have been collected as part of the studies for the reclamation of the Bagnoli area in Naples.

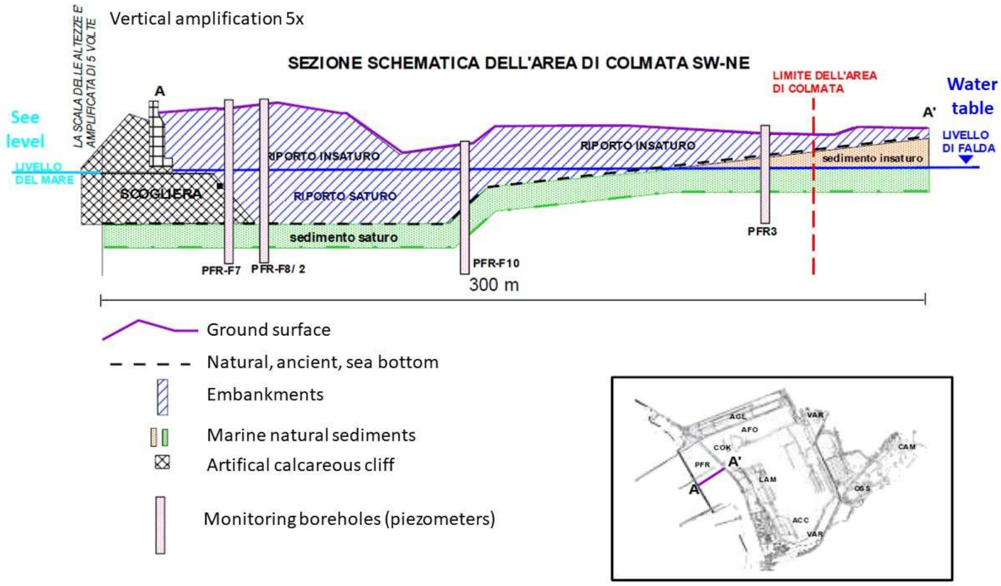

Figure 3.2: Schematic section of the reclaimed area.

Data on the coastal aquifer

Data are found in the `Bagnoli.xls` file.

In order to evaluate tidal effects on the water level of the aquifer, the depths of the water table were measured on March 5, 2002, for a period of about 10 hours, in some piezometers located in the reclaimed area at different distances from the coast line. These data can be found in sheet "`Survey 05-03-2002`".

Data in sheet "`PFRN24 26-03-2001`" refer to the measurements for a period longer than 24 hours starting from March 26, 2001, in the PFRN24 piezometer.

Location of piezometers

PFRF7 is about 25 m from the coastline, PFR-F 8/2 about 35 m, PFR-F 10 about 125 m, PFR3 about 250 m. On the other hand, PFRN24 piezometer is located about ten meters from the shoreline outside the reclaimed area. From a geological point of view, the piezometers located in the reclaimed area cross the embankment and then the soil lithotype, with the exception of PFR-F7 which, below the embankment layer, also crosses the artificial cliff that delimits the boundary of the reclaimed area (see figure 3.2).

Sea level data

In sheets "`LIV 26-28 March 2001`" and "`LIV 2-8 March 2002`", data recorded by the tide gauge station of Naples of the national tide gauge network (National Mareographic Network[1]) are reported. In particular, the first sheet shows the sea level measured on 26, 27 and 28 March 2001 and the second sheet shows the sea level measured from 2 to 8 March 2002.

[1]`http://www.mareografico.it/`

3.2.2 Questions and suggestions

1. Draw graphs of the trends of the various variables and comment the results.
2. Considering a 1-D water flow in the aquifer, in a direction perpendicular to the coast, solve the flow equation for a sinusoidal time-varying boundary condition (in analogy to the solution of the heat equation for surface temperature variations shown in 3.2.3).
3. Is it possible to determine some of the physical parameters of the aquifer (T and/or S) from the phase shift and amplitude of the oscillations of the piezometric level in relation to the oscillations of the sea level?

3.2.3 Propagation of the surface fluctuations of temperature

Temperature at the ground surface is largely controlled by climatic and meteorological factors. Therefore, the variation of temperature with time can be approximated as a cosine function with a given period T:

$$T(0,t) = T_0 + \Delta T \cos(\omega t), \tag{3.10}$$

where $\omega = 2\pi/\mathrm{T}$ and T_0 takes into account the effects of all the other sources and boundary conditions, which are not related to the periodic, harmonic oscillation of temperature at the ground surface. The heat equation, for a homogeneous medium, if convection and heat production is negligible and if one–dimensional vertical heat flow only is considered, is given by

$$\frac{\partial T}{\partial t} = \kappa \frac{\partial^2 T}{\partial z^2}, \tag{3.11}$$

where κ is the thermal diffusivity. A solution to this equation can be searched with the method of separation of the variables, i.e., in the following form:

$$T(z,t) = T_0 + c\mathcal{Z}(z)\mathcal{T}(t). \tag{3.12}$$

If the time and space derivatives are computed and inserted in (3.11), the following equation is obtained:

$$\mathcal{Z}(z)\mathcal{T}'(t) = \kappa\mathcal{T}(t)\mathcal{Z}''(z),$$

which can be expressed as

$$\frac{\mathcal{T}'}{\mathcal{T}}(t) = \kappa\frac{\mathcal{Z}''}{\mathcal{Z}}(z) = \alpha, \tag{3.13}$$

where α is a constant value, independent of both z and t.

Therefore $\mathcal{T}(t) = \exp(\alpha t)$ and $\mathcal{Z}(z) = \exp(ikz)$. The value of k is fixed by substituting the expression of $\mathcal{Z}(z)$ in (3.13): $k^2 = -\alpha\kappa^{-1}$. Therefore the tentative solution (3.12) attains the expression

$$T(z,t) = T_0 + c\exp(ikz)\exp(\alpha t). \tag{3.14}$$

Since, from (3.10), $T(0,t)$ can be interpreted as the real part of $T_0 + \Delta T \exp(i\omega t)$, then $c = \Delta T$ and $\alpha = i\omega$, so that $k = \sqrt{-\alpha/\kappa} = \sqrt{\omega/\kappa}\cdot\sqrt{-i}$ and (3.14) becomes

$$T(z,t) = T_0 + \Delta T \exp\left(i\sqrt{\omega/\kappa}\cdot\sqrt{-i}z\right)\exp(i\omega t). \tag{3.15}$$

Since $i = \exp(i(3\pi/2 + 2n\pi))$ and $\sqrt{-i} = \exp(i(3\pi/4 + n\pi))$, where n is an integer, either

$$\sqrt{-i} = \frac{-1+i}{\sqrt{2}}, \tag{3.16}$$

or

$$\sqrt{-i} = \frac{1-i}{\sqrt{2}}. \tag{3.17}$$

If (3.16) is used in (3.15), then

$$T(z,t) = T_0 + \Delta T \exp\left(\frac{-i-1}{\sqrt{2}}\sqrt{\frac{\omega}{\kappa}}z + i\omega t\right) = T_0 + \Delta T \exp\left[-\sqrt{\frac{\omega}{2\kappa}}z + i\left(\omega t - \sqrt{\frac{\omega}{2\kappa}}z\right)\right].$$

In this case, at large depth, i.e., for $z \to -\infty$, the first exponential increases indefinitely and therefore, this solution is not physically consistent.

Instead, if (3.17) is used in (3.15), then

$$T(z,t) = T_0 + \Delta T \exp\left(\sqrt{\frac{\omega}{2\kappa}}z\right) \exp\left[i\left(\omega t + \sqrt{\frac{\omega}{2\kappa}}z\right)\right]. \tag{3.18}$$

This solution shows that the periodic oscillations of temperature at the ground surface propagate into depth, by reducing their amplitudes exponentially. The "damping" depth scale is given by $\sqrt{2\kappa/\omega}$.

Moreover, the oscillations follow an harmonic behavior, but with a phase shift that is proportional to the depth.

CHAPTER 4

Exercises on ocean circulation, waves and tides

4.1 Differential operators

4.1.1 Exercise on differential operators of simple vector fields

Draw the velocity fields listed in Table 4.1. For each of them compute the divergence and the curl and comment the results from the physical point of view.

Which of these fields corresponds to an incompressible flow?

Which of these fields can be expressed with a velocity potential ($\mathbf{v} = \mathrm{grad}\phi$)?

Linear velocity field	$\mathbf{v} = (y, 0, 0)^t$
Diverging velocity field	$\mathbf{v} = \begin{pmatrix} x \cdot \left(x^2 + y^2 + z^2\right)^{1/2} \\ y \cdot \left(x^2 + y^2 + z^2\right)^{1/2} \\ z \cdot \left(x^2 + y^2 + z^2\right)^{1/2} \end{pmatrix}$
Rotating velocity field	$\mathbf{v} = (-y, x, 0)^t$

Table 4.1: Velocity fields.

4.1.2 Vector potential

Let $\phi(x, y, z) = x^2 + y^2 + z^2$ be the velocity potential. Compute and draw the corresponding vector field ($\mathbf{v} = \mathbf{grad}\phi$). Compute the divergence and the curl of the obtained velocity field and comment the result from the physical point of view.

4.2 Waves

4.2.1 Exercise on dispersion relationships

Consider the equations and the plane wave solutions listed in Table 4.2. Determine for each of them the dispersion relation, i.e., the dependence of ω on k or $\mathbf{k}$, and the phase velocity.

Equation	Wave function
$\dfrac{\partial \phi}{\partial t} + c\dfrac{\partial \phi}{\partial x} = 0$	$\phi(x,t) = \exp(\iota(kx - \omega t))$
$\dfrac{\partial^2 \phi}{\partial t^2} - c\dfrac{\partial^2 \phi}{\partial x^2} = 0$	$\phi(x,t) = \exp(\iota(kx - \omega t))$
$\dfrac{\partial \phi}{\partial t} + \mathbf{c} \cdot \mathbf{grad}\phi = 0$	$\phi(\mathbf{x},t) = \exp(\iota(\mathbf{k} \cdot \mathbf{x} - \omega t))$

Table 4.2: Wave equations and plane waves.

4.2.2 Reflection of sea waves

Consider the case of an horizontal sea bottom close to a vertical cliff. What do you expect if sea waves hit the cliff with a given incidence angle?

4.3 Tides

4.3.1 Field data analysis

Download the data for some stations from the Sea level station monitoring facility of UNESCO[1]; it is suggested to download data for a time interval of 30 days.

Perform a spectral analysis to find the typical periods (T) of tides. It is suggested to select at least three stations from different oceanographic conditions (e.g., different oceans or closed basins; different latitudes), taking into account the maps of the M2 and K1 components shown during the lectures. Consider also the comparison of the results for different time intervals (e.g., one month in summer and one in winter). Comment the results.

[1] See `http://www.ioc-sealevelmonitoring.org/map.php`.

Bibliography

P.R. Bevington. *Data reduction and error analysis for the physical sciences.* McGraw-Hill, 1969.

R.H. Stewart. *Introduction to Physical Oceanography.* University Press of Florida, 2009.

G.C. Topp, J.L. Davis, and A.P. Annan. Electromagnetic determination of soil water content: Measurements in coaxial transmission lines. *Water resources research*, 16(3):574–582, 1980.

Credits

In this section, appropriate credits are given to the sources from which some of the pictures have been taken.

Figure 1.2 From `https://www.powerstream.com/how-to-measure-current.htm`.

Figure 2.2 Used under CC-BY-SA 3.0, retrieved from `https://en.wikipedia.org/wiki/CTD_(instrument)#/media/File:CTDdeploy.jpg`.

Figure 2.3 Retrieved from `https://it.wikipedia.org/wiki/File:Niskin-bottle.jpg` and Stewart (2009).